

A Novel Approach for Predicting Particulate Matter 2.5 and 10 Concentration using Modal Autoformer and Seq-2Seq Model

Rajendran Thavasimuthu ¹, Vidhya PM², Arulkumar Varatharajan^{*3}, Sridhar Sekar⁴, Ashokkumar Sighamani⁵, Ajay Kumar Yadav⁶

¹Department of Sustainable Engineering, Saveetha School of Engineering, Saveetha Institute of Medical and Technical Sciences, Chennai, Tamilnadu, India. rajendran.thavasimuthusamy@gmail.com

²Department of Information Technology, Rajagiri School of Engineering and Technology, Kochi, Kerala, India. vidhya_pm@proton.me

³Department of Database Systems, School of Computer Science and Engineering, Vellore Institute of Technology, Vellore, Tamil Nadu, India. arulkumaran.ckpc@gmail.com, +91 94860 78445

⁴Department of Research, Rajalakshmi Institute of Technology, Chennai, Tamilnadu, India. sridhar.sse@protonmail.com

⁵Department of Computer Science and Engineering, Saveetha School of Engineering, Saveetha Institute of Medical and Technical Sciences, Chennai, Tamilnadu, India. ashokkumar_sse@proton.me

⁶Department of Computer Application, United Institute of Management, Allahabad, Uttar Pradesh, India. ajaykumar.uim@gmail.com

*Corresponding author: arulkumaran.ckpc@gmail.com

1 Graphical Abstract



2 |

3 **Abstract:** Precise and dependable forecasting of Particulate Matter 2.5 ($PM_{2.5}$) and PM_{10} levels hold
4 significant importance for the public's ability to proactively mitigate exposure to air pollution and for
5 informing governmental policy responses. Nonetheless, predicting $PM_{2.5}$ and PM_{10} concentrations
6 presents considerable challenges due to the complex dynamics of atmospheric flows. In existing
7 mainstream research, most air pollution prediction models presently employ a single predictor, hence
8 limiting the potential for enhancing stability and accuracy. This study proposes a pioneering
9 methodology for forecasting $PM_{2.5}$ and PM_{10} concentration levels by integrating a Modal Auto former
10 system with the Sequential-to-Sequential predictive model. The Seq-2Seq network model leverages
11 sequential learning and square transformation of Long Short-Term Memory (LSTM) techniques for
12 improved accuracy in $PM_{2.5}$ and PM_{10} concentration prediction. Additionally, the incorporation of a
13 Modal Auto former enhances the predictive capabilities by efficiently capturing nuanced variations in
14 atmospheric conditions. The proposed Seq-2Seq LSTM network predictor is given a weight, and the
15 Adaptive Beetle Feelers Optimization (ABFO) algorithm is utilized for weight optimization to attain
16 the best prediction results. Through rigorous experimentation and validation, the proposed approach
17 demonstrates superior performance compared to traditional methods using Air Quality Data in India
18 from Kaggle, offering a promising avenue for precise $PM_{2.5}$ and PM_{10} concentration forecasting with
19 practical implications for air quality management and public health initiatives. The Proposed seq-2seq
20 LSTM model achieved 10.211 RMSE for $PM_{2.5}$, 10.321 RMSE for PM_{10} , 5.641 MAE for $PM_{2.5}$,
21 5.764 MAE for PM_{10} , 0.976 R^2 for $PM_{2.5}$, and 0.945 R^2 for PM_{10} .

22 **Keywords:** Air Quality, Adaptive Beetle Feelers Optimizer, Deep learning, Modal Auto Former, PM
23 Concentration Forecasting.

24 1. INTRODUCTION

25 The exponential growth of the world's economy has increased concerns pertaining to the issue
26 of air pollution [1]. Exhaust emissions, primarily resulting from the burning of fossil fuels, have
27 significantly contributed to an increase in atmospheric pollutants. The term $PM_{2.5}$ refers to particulate
28 matter that has a diameter of 2.5 micrometres or less. These small, lightweight, and inhalable
29 pollutants can last in the atmosphere for prolonged periods and provide a substantial risk to human
30 health when found in substantial amounts. The World Health Organization (WHO) suggests that the
31 average annual $PM_{2.5}$ concentrations should not surpass $5 \mu\text{g}/\text{m}^3$. The primary contributors of $PM_{2.5}$

emissions are the combustion of solid waste, road vehicles, and power plants [2]. As per the WHO, the global yearly mortality rate associated with air contamination is estimated to be more than seven million, and this rate is steadily increasing. WHO states that PM is a widely used proxy measure for air pollution. There exists substantial data supporting the adverse health effects linked to exposure to this contaminant. Sulfate, nitrates, ammonia, sodium chloride, black carbon, mineral dust, and water are the primary constituents of PM [3].

The top five countries with the highest levels of pollution in 2023 were:

- Bangladesh's $PM_{2.5}$ concentration ($79.9 \mu\text{g}/\text{m}^3$) exceeds the WHO $PM_{2.5}$ yearly limit by more than 15 times. Bangladesh's elevated pollution levels can be attributed to the country's continuous traffic, construction operations, and industrial emissions, specifically from brick kilns that heavily depend on coal.
- Pakistan's $PM_{2.5}$ concentration ($73.7 \mu\text{g}/\text{m}^3$) exceeds the WHO $PM_{2.5}$ yearly limit by more than 14 times.
- India's $PM_{2.5}$ concentration ($54.4 \mu\text{g}/\text{m}^3$) exceeds the WHO $PM_{2.5}$ yearly limit by more than tenfold.
- Tajikistan's $PM_{2.5}$ concentration ($49.0 \mu\text{g}/\text{m}^3$) exceeds the WHO $PM_{2.5}$ yearly limit by more than 9 times.
- The $PM_{2.5}$ concentration in Burkina Faso ($46.6 \mu\text{g}/\text{m}^3$) exceeds the WHO $PM_{2.5}$ yearly limit by more than 9 times.

Out of a total of 134 nations and regions, 124 (92.5%) surpassed the annual $PM_{2.5}$ recommendation value of $5 \mu\text{g}/\text{m}^3$ set by the WHO.

53

1.1. Air Pollution in India

India is one of the most rapidly expanding economies globally; however, its rapid process of urbanization and industrialization has had adverse effects on the country's environment and the well-being of its citizens. The country has seen significant water pollution, soil degradation, and poor air quality due to human activities, resulting in a substantial number of premature deaths annually. In the year 2023, New Delhi emerged as the capital city with the highest level of pollution globally, as evidenced by its average $PM_{2.5}$ concentration of $92.7 \mu\text{g}/\text{m}^3$. Subsequently, the capital city of Bangladesh, Dhaka, followed. Begusarai, located in northeastern India, has the highest $PM_{2.5}$ levels globally, with an average $PM_{2.5}$ concentration of around $119 \mu\text{g}/\text{m}^3$.

The monthly $PM_{2.5}$ concentrations in urban areas of India exhibited comparable trends from 2020 to 2023, with the winter months consistently exhibiting the greatest concentrations. During the specified time frame, the city of Delhi had the highest mean $PM_{2.5}$ concentration, surpassing $255 \mu\text{g}/\text{m}^3$ in November 2023. According to data from 2023, Delhi had the third-highest mean $PM_{2.5}$ concentration among cities in India, ranking below Begusarai and Guwahati. The prevalence of severe air pollution in India might have adverse health consequences for the nation's populace. Fine particulate contaminants can extensively infiltrate the pulmonary system, leading to respiratory complications and perhaps leading to premature mortality. By 2022, almost 96 percent of India's inhabitants were subjected to hazardous levels of atmospheric contamination as shown in Figure 1.

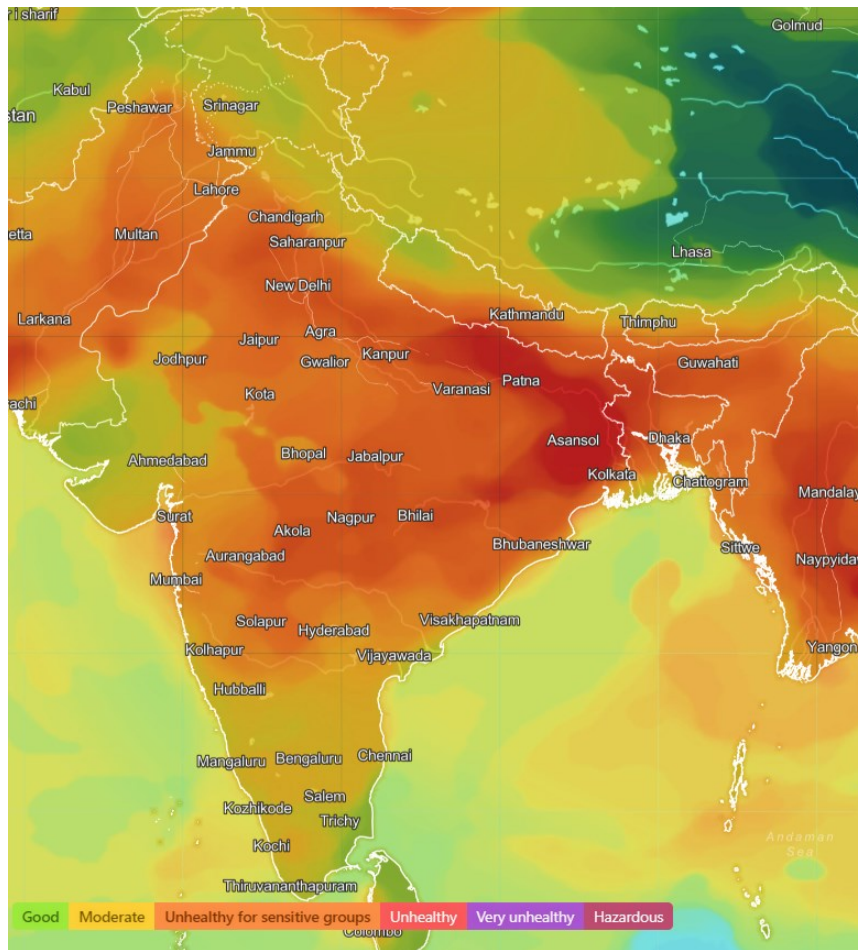


Figure 1. Map View of Air Quality in India (March 2024)

72

73

74 PM10 aerosols, which are PM with a size of 10 μm or less, are a kind of air pollutant that contributes
 75 to the decline in air quality. PM10 originates from a combination of natural and human activities, and
 76 its constituents are classified as primary (emitted directly) and secondary (produced in the
 77 atmosphere) in the natural environment. A considerable proportion of PM10 sources can be attributed
 78 to human activities. Several variables influence atmospheric PM10 concentrations, including local
 79 sources, dispersion, transportation, land-use patterns, geography, and meteorological conditions. The
 80 ambient air concentration of PM10 in Delhi, India's capital, was recorded at 181 micrograms per
 81 cubic meter in 2021. The pollutant levels remained consistently elevated for more than ten years. A
 82 higher quantity of particulate matter in the atmosphere has been linked to a wide range of physical,
 83 environmental, and health problems.

84 Fine particulate matter (PM2.5) and Inhalable particulate matter (PM10), which have aerodynamical
 85 dimensions lower than 10 and 2.5 μm , are widely recognized as significant pollutants [4]. Increased
 86 levels of PM2.5 and PM10 in the environment provide substantial health hazards, which may result in
 87 respiratory infections and conditions related to cardiopulmonary dysfunction, hence providing serious
 88 consequences to human health [5].

89 The precise prediction of air pollution provides significant early indicators and assists in the decision-
 90 making process for both governmental and public entities in addressing instances of severe pollution
 91 [6,7]. Hence, there is a pressing requirement for reliable and accurate prediction of ambient PM2.5
 92 and PM10 levels to improve air quality and protect public health. The accurate forecasting of PM
 93 levels, including PM10 and PM2.5, over an extended period is an essential element in endeavours to
 94 comprehend and address the widespread problem of air pollution. PM comprises microparticles
 95 floating in the atmosphere and originates from several origins including automotive emissions,
 96 industrial operations, construction activities, and natural occurrences such as dust storms and

97 wildfires. The presence of these particles presents notable health hazards due to their ability to
98 infiltrate the respiratory system, resulting in respiratory and cardiovascular ailments, alongside several
99 other harmful health consequences.

100 The significant threat posed by air pollution, particularly the concentrations of PM_{2.5} and PM₁₀, to
101 public health and environmental sustainability is acknowledged. Accurate forecasting of these
102 concentrations is considered crucial for proactive mitigation strategies and informed policy responses.
103 However, limitations in accuracy and stability are often encountered by existing forecasting models
104 due to the complexities of atmospheric processes. It is observed that traditional forecasting
105 approaches typically rely on single predictors, which may not adequately capture the intricate
106 interactions that drive air pollution dynamics. Consequently, a pressing need is identified for novel
107 methodologies that can improve the precision and reliability of PM_{2.5} and PM₁₀ concentration
108 forecasts. This research addresses this need by proposing a novel methodology that integrates a Modal
109 Autoformer system with a Seq-2-Seq predictive model. This innovative approach is intended to
110 overcome the shortcomings of traditional forecasting methods by leveraging advanced techniques in
111 sequential learning and optimization.

112 The novelty of this research present in the integration of a Modal Auto-former system with a Seq-
113 2Seq LSTM network, enhanced by ABFO for weight optimization. Unlike traditional models that rely
114 on single predictors, this approach captures complex atmospheric dynamics and variations in PM
115 levels, significantly improving the accuracy and stability of PM_{2.5} and PM₁₀ forecasting, as
116 validated on Indian air quality data. By combining the capabilities of the Seq-2-Seq model with the
117 nuanced insights provided by the Modal Autoformer, the proposed methodology aims to increase the
118 accuracy and robustness of PM_{2.5} and PM₁₀ concentration anticipation. Furthermore, the utilization
119 of the ABFO algorithm for weight optimization is intended to further refine the forecasting process,
120 enabling more precise estimations of air pollutant levels. Through experimentation and validation
121 using real-world Air Quality Data from India, the research seeks to indicate the superior performances
122 of the research model to the conventional approaches. By providing a more reliable means of
123 forecasting PM_{2.5} and PM₁₀ concentrations, the developed methodology has the potential to have
124 significant implications for air quality management and public health initiatives.

125 The main contributions of this work are:

- 126 • The study proposes a novel methodology by integrating a Modal Autoformer system with the
127 Seq-2Seq predictive model. This integration aims to increase the accuracy of forecasting
128 PM_{2.5} and PM₁₀ contamination levels.
- 129 • Incorporating a Modal Autoformer to further enhance the predictive capabilities of the model
130 by efficiently capturing nuanced variations in atmospheric conditions. This enables the model
131 to capture subtle changes in atmospheric dynamics, leading to more accurate predictions.
- 132 • Employing the ABFO algorithm to optimize the weights of the proposed predictor. This
133 adaptive optimization approach dynamically adjusts the weights based on the model's
134 performance, leading to improved forecasting results.
- 135 • Through rigorous experimentation and validation using Air Quality Data from Kaggle, the
136 proposed approach demonstrates superior performance compared to traditional methods. The
137 improved accuracy of PM_{2.5} and PM₁₀ concentration prediction offers a promising avenue
138 for precise air quality management and public health initiatives.

139 Section 2 describes the research data and methodology. The research methodology is evaluated and
140 explained in section 3. Finally, the work is concluded.

141 2. LITERATURE REVIEW

142 There are three main categories of existing approaches used for predicting air pollution
143 concentrations: numerical models, statistical models, and artificial intelligence (AI) techniques.
144 Numerical models are utilized to replicate the intricate differential equations that control the physical
145 and chemical mechanisms of pollutants present in the atmosphere. Notable instances of such models
146 encompass Weather Research and Forecasting coupled with Chemistry (WRF-Chem) and Community

147 Multi-scale Air Quality (CMAQ). Nevertheless, the efficacy of these models is strongly dependent on
148 comprehensive and frequently conflicting pollutant emission data, necessitating significant
149 computational resources due to their intricate nature. On the other hand, statistical models like
150 autoregressive integrated moving average (ARIMA) and autoregressive moving average (ARMA)
151 rely on data and need minimal processing resources. However, they may encounter difficulties when
152 dealing with nonlinear relationships and stationary data assumptions. AI models, such as artificial
153 neural networks (ANN), random forest (RF), extreme gradient boosting (XGB), and support vector
154 regression (SVR) have the capability to effectively capture intricate nonlinear relationships. However,
155 these methods frequently need manual feature engineering and may encounter difficulties when
156 dealing with extensive datasets because of data redundancy problems. Deep learning (DL) algorithms
157 have recently gained attention as a possible method for predicting air pollution. This is because they
158 possess the ability to learn on their own and effectively handle intricate nonlinear mappings.

159 Zhang et al. [8] provided a reliable prediction method that enables precise multi-steps forward
160 forecasting of PM10 and PM2.5 levels. Following this, the corrected inputs were modelled using the
161 convolution neural networks (CNN) based on residuals and has the ability to extract features.
162 Ultimately, the effectiveness of this system was thoroughly evaluated by using five accuracy measures
163 and two extra statistical tests. The STA-ResCNN model demonstrated a significant reduction in root
164 mean square error (RMSE), ranging from 5.595% to 15.247% and 6.827% to 16.906%, for the
165 average of 1- to 4-hour forward forecasts of PM2.5 and PM10 in three prominent cities, respectively.
166 Yu et al. [9] provided a DL architecture called SpatioTemporal (ST)-Transformer, which utilized
167 multi-head attention. The purpose of this design was to enhance the accuracy of spatiotemporal
168 forecasts for PM2.5 concentration in areas exposed to wildfires. This model utilized the sparse
169 attention method that focused on useful data across variable, temporal, and spatial dimensions.

170 Faraji et al., [10] introduced a model that integrated 3D CNN and GRU to predict the concentration of
171 PM2.5 on an hourly and daily basis. The model demonstrated superior performance in comparison to
172 ANN, GRU, LSTM, ARIMA, and SVR. Ding et al. (2011) proposed a CNN-LSTM method to predict
173 PM2.5 concentrations by leveraging spatiotemporal correlations. The methods were utilized for
174 extracting the spatial characteristics and temporal relationships of the inputs. The method
175 demonstrated superior performances than the multilayers perceptron (MLP) and individual LSTM
176 models. The accuracy of prediction was improved by including spatiotemporal correlation.

177 The spatial and temporal information were gathered using either a CNN or DNN architecture in [12]
178 and [13]. In brief, the models possessed notable capabilities in their capacity to integrate geographical
179 and temporal data, hence enabling precise prediction of PM2.5 air quality and concentration.
180 Nevertheless, the majority of the models exhibited limitations in terms of short-term projections, with
181 many models being restricted to certain locations or contaminants. Moreover, certain models may
182 incur significant computing costs because of their intricate designs. Additional investigation was
183 required to cultivate more effective and precise models that can be implemented on a broader scope.
184 The study [14] introduced a balanced methodology of sampling to mitigate the issue of unbalanced
185 data to increase the accuracy of PM2.5 prediction. Most enhancements derived from the LSTM
186 architecture mostly focussed on feature extraction.

187 The research in [15] employed the BiLSTM method, which deviated from conventional LSTM by
188 incorporating two distinct hidden layers to process the sequences in both the backward and forward
189 directions. This approach effectively addressed the temporal and spatial correlations presented in the
190 information and facilitated the modelling of intricate nonlinear associations within meteorological
191 factors and air quality parameters. The study [16] employed a hybrid approach using principal
192 component analysis (PCA), an attention mechanism, and long short-term memory (LSTM). Peralta et
193 al., [17] provided a technique that utilized the LSTM recurrent network model to forecast the
194 concentration of PM2.5 at any given geographical location. This method can forecast PM2.5
195 concentration for the upcoming day in a newer place where data were unavailable by considering air
196 pollutant historical values and meteorological parameters (wind speed, temperature, relative humidity,
197 and direction) assessed at stations fixed for monitoring.

198 The research in [18] introduced the CE-AGA model, which integrated the attention-based GRU with
 199 the convolutional encoders with adaptive gated activations. This model was specifically designed for
 200 predicting air quality. Several studies have employed transfer learning techniques to exploit pre-
 201 trained methods for associated operations, hence enhancing the efficacy of prediction models. The
 202 LSTM model was employed by Gul et al. [19] and Waseem et al. [20], who employed both partial
 203 fine-tuning of the parameters or structure. The utilization of the LSTM model facilitated the
 204 representation of temporal relationships, while the extensive array of trials conducted on diverse real-
 205 time monitoring of air quality data sets from many stations enhanced the applicability of the findings.
 206 Nevertheless, many research works failed to offer a comprehensive examination of the LSTM model's
 207 interpretability or the characteristics it acquired from air pollutant data were crucial for predicting
 208 based on DL models.

209 The methodology presented by Wang et al. [21] utilized LSTM, RF, and PSO. Particle Swarm
 210 Optimization (PSO) facilitated rapid convergence of the model to the optimal solutions, especially in
 211 search space with a high number of dimensions and intricate, nonlinear interactions among variables.
 212 The integration of PSO and ESN has the potential to achieve superior performance in the prediction of
 213 time series by capitalizing on ESN's proficiency in handling sequential information and PSO's test in
 214 conducting global search. The research in [22] proposed a DL hybrid approach that integrated the
 215 Particle Swarm Optimization and slime mould algorithm (SMA) into the adaptive neuro-fuzzy
 216 inferences system (ANFIS) for predicting PM2.5 levels.

217

Table 1. Analysis of Reviewed Studies

Study	Approach	Application	Advantages	Disadvantages
[8]	Residual-based CNN with feature extraction	PM10 and PM2.5 prediction	- Improved accuracy - Comprehensive assessment of performance	- Computational complexity - Reliance on detailed pollutant emission data
[9]	Multi-head attention-based deep learning	Spatiotemporal predictions of PM2.5 concentrations in wildfire-prone areas	- Sparse attention mechanism for useful contextual information	- Limited to specific scenarios - May require large datasets to train effectively
[10]	3DCNN-GRU	PM2.5 concentration forecasting	- Best results compared to other models	- Computational complexity
[11]	CNN-LSTM	PM2.5 prediction based on spatiotemporal correlations	- Enhanced prediction accuracy through spatial and temporal feature extraction	- Complexity in architecture
[12]; [13]	CNN or DNN architecture	PM2.5 concentration predictions	- Incorporates temporal and spatial data for precise predictions	- Limited to short-term predictions - Computational expense due to complex architectures
[14]	LSTM with a balanced sampling approach	PM2.5 concentration prediction with imbalanced data	- Addresses imbalanced data for improved prediction	- Limited analysis of interpretability - Complexity in feature extraction
[15]	BiLSTM model	Handling temporal and spatial correlations in data for air pollution prediction	- Handles spatial and temporal correlations effectively	- Computational complexity
[16]	PCA, attention mechanism, LSTM	PM2.5 concentration prediction with feature extraction and attention mechanism	- Incorporates principal component analysis for feature reduction - Attention mechanism for improved focus on relevant features	- Complexity in architecture

[17]	LSTM recurrent network model	Space-time prediction of PM2.5 concentration considering historical air pollutant and meteorological data	- Predicts PM2.5 concentrations at new locations using historical data	- Relies on the availability of historical data - Limited to fixed monitoring station locations
[18]	Attention-based GRU and convolutional encoder	Air quality prediction using adaptive gated activation and transfer learning	- Utilizes attention mechanism and transfer learning for improved prediction	- May require large datasets for transfer learning - Computational complexity
[19]; [20]	LSTM model	Air quality prediction using LSTM neural networks	- Models temporal dependencies effectively - Generalizable results due to experiments on multiple datasets	- Limited interpretability of the LSTM model - Complexity in training and tuning parameters
[21]	LSTM, RF, PSO	PM2.5 prediction using PSO, RF, LSTM.	- PSO aids in fast converging to optimal solutions - Combined strengths of PSO and ESN for time series forecast.	- Computational complexity
[22]	DL hybrid method	PM2.5 prediction using SMA, PSO, and ANFIS	- Novel hybrid model for PM2.5 predictions	- Complexity in combining different algorithms

218

219 From the above review, Traditional methods struggle for capturing the complex, nonlinear relations
220 between input variables and PM concentrations. LSTM can automatically extract relevant features
221 from raw data, learning complex representations that improve prediction accuracy. However, LSTMs
222 are more computationally expensive compared to simpler recurrent architectures like the Elman RNN
223 due to their additional gating mechanisms and cell state management. These increased complexities
224 could result in longer training period and higher resource demand, making them less suitable for
225 deployment on resource-constrained devices or in real-time applications. To solve this, the seq-2seq
226 model is introduced here to improve the PM concentration prediction accuracy.

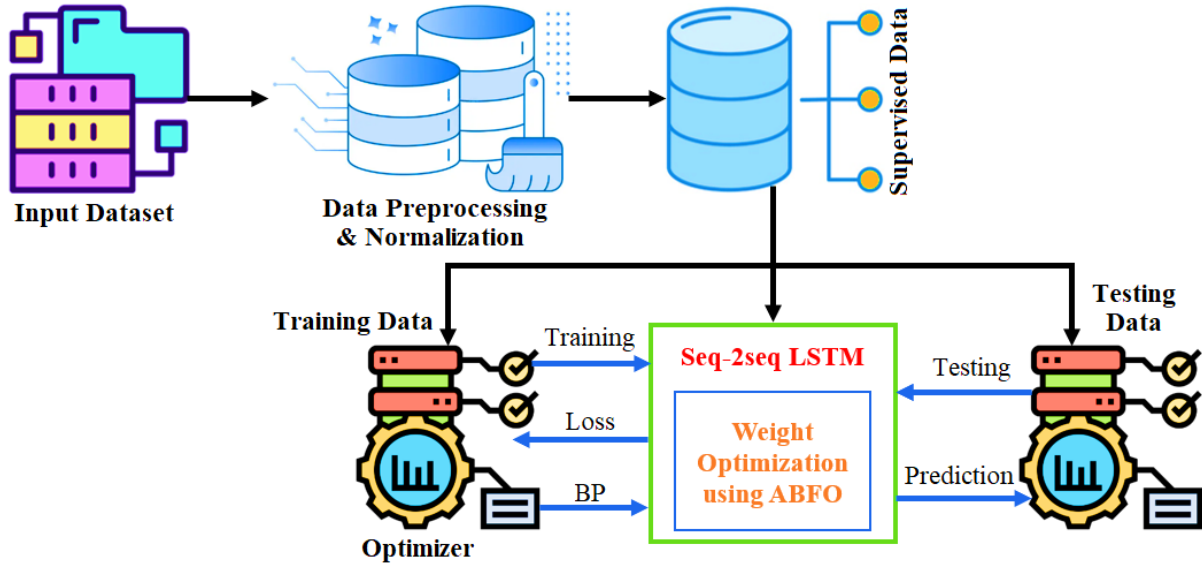
227 2.1. Research Gap

228 The research into PM2.5 and PM10 forecasting has predominantly concentrated on predictive
229 modelling and algorithmic optimization, although it is lacking in an integrated combination of
230 approaches that consider pollutant emission characteristics, spatial distribution dynamics, and real-
231 world fuel impact analyses. Analyses of the morphology and nanostructure of emissions, as examined
232 in studies of air pollution production, alongside the reduction properties of sustainable aviation fuels,
233 may enhance comprehension of pollutant sources and variability [Chen et al. 2024; Gong et al. 2024;
234 Meng et al. 2023; Xu et al. 2024]. Furthermore, employing methods for effective small-target
235 identification in noisy environments and comprehending the factors influencing spatial pollutant
236 distribution could improve the precision of forecasting models by addressing the complexities of
237 dynamic atmospheric conditions and varied pollutant sources. This highlights the necessity of
238 incorporating advanced emission analysis, spatial dynamics, and robust detection approaches into PM
239 forecasting systems to effectively address these gaps.

240 3. RESEARCH METHODOLOGY

241 The proposed model employs a Seq-2seq LSTM network architecture to forecast the PM2.5
242 and PM10 concentrations, as seen in Figure 2. Initially, the Kaggle dataset is subjected to pre-
243 processing procedures, which involve filling in missing values and normalizing the data.
244 Subsequently, the dataset is divided into training and test sets to facilitate model training and
245 assessment. During the training process, the Seq-2seq LSTM model is trained using each batch of

246 training data for a predetermined number of iterations. The loss value during forward propagation
 247 inside the network is minimized by employing the Adaptive Beetle Feelers Optimization (ABFO)
 248 technique via backpropagation. After training, the test data is loaded into the seq-2seq LSTM model to
 249 get predicted values for PM2.5 and PM10. To acquire the actual expected values, the predictions are
 250 de-normalized. Ultimately, the efficiency of the seq-2seq LSTM model is assessed using diverse
 251 measures, whereby the actual projected values are compared with the true values.



252
 253 **Figure 2. Seq-2seq LSTM-based PM concentration prediction**

254 **3.1. Dataset Collection**

255 The dataset was obtained from the website [https://www.kaggle.com/datasets/fedesoriano/air-](https://www.kaggle.com/datasets/fedesoriano/air-quality-data-in-india)
 256 [quality-data-in-india](https://www.kaggle.com/datasets/fedesoriano/air-quality-data-in-india) Fedesoriano (2022). Providing data on significant air pollutants like particle
 257 matter (PM2.5 and PM10), carbon monoxide (CO), sulfur dioxide (SO2), nitrogen dioxide (NO2), and
 258 ozone (O3), across several cities in India. The dataset often contains timestamps that correlate to the
 259 day and time of measurement, as well as pollutant concentrations measured in quantities such as
 260 micrograms per cubic meter ($\mu\text{g}/\text{m}^3$). This dataset is an essential source for analysts and researchers to
 261 analyze air quality trends, investigate the impact of pollution on public health, develop predictive
 262 models for predicting air quality, and evaluate the effectiveness of air quality management strategies
 263 and policies. The metadata includes information on monitoring locations and quality control. The map
 264 view of monitoring stations in India is displayed in Figure 2.

265 **3.2. Data Pre-processing**

266 The proposed approach considers the prediction of PM2.5 as a regression issue of time series,
 267 requiring continuous time series data as input. Still, it is frequently observed in practical situations
 268 that there are disruptions in the chronological order of data, resulting in the presence of data gaps. The
 269 issue pertaining to the absence of multi-modal and multi-site air quality information can be classified
 270 into two distinct classes: the complete absence of time series recordings, and the absence of feature
 271 values within individual records. Missing data-filling software mostly uses functional design to
 272 address the two categories of missing data. To address missing values in PM concentration data, this
 273 system must calculate the coefficients of cubic polynomials that interpolate between neighbouring
 274 known data points using cubic spline interpolation. The polynomials are subsequently employed to
 275 approximate the absent values.

276 The proposed approach produces cubic spline functions for every interval p_i, p_{i+1} using the known
 277 data points specified as p_i, q_i , where p_i indicates the time points and q_i indicates the PM
 278 concentration values.

279
$$CS_i(p) = w_i(p - p_i)^3 + (p - p_i)^2 + y_i(p - p_i) + z_i \quad (1)$$

280 The coefficients w_i, x_i, y, z_i need to be calculated. The original dataset was filled with missing values
 281 and subsequently normalized. Min-max scaling is a method that adjusts the data to fit inside the
 282 predetermined level, usually ranging from 0 to 1. The Min-Max scaling formula is as follows:

$$283 \quad P_n = \frac{P - P_{min}}{P_{max} - P_{min}} \quad (2)$$

284 Here, P represent the initial PM concentration value, P_n represent the normalized value of P , and P_{max}
 285 and P_{min} indicate the highest and lowest values of P in the dataset. Autoformer is a transformer-based
 286 DL model. The system comprises an internal sequences decomposition unit, an enhanced
 287 decomposition structure based on the encoder-decoder, and a self-correlation mechanism. The
 288 decomposition unit utilizes the sliding average concept to extract and deconstruct the seasonal
 289 elements of time-series information. The primary aim of this process was to examine the intricate
 290 temporal patterns exhibited by a lengthy time series. To mitigate periodic oscillations and emphasize
 291 enduring trends, moving average lines are strategically incorporated. The incorporation of the sliding
 292 average effects will be accomplished by the sliding average window size manipulation.

293 3.3. Seq-2seq LSTM Model for PM Prediction

294 To acquire the time sequence attention of the multi-variable input data, the module of time
 295 sequence attention was employed to examine the various time data steps. Next, the input should be
 296 updated, and feature coding should be performed based on the attention received for each input data.
 297 The final projected value is obtained by fusing the matrix of encoded features with the historic data of
 298 PM2.5 concentrations and inputting it into the decoding features for decoding. A solitary LSTM unit
 299 consists of a memory cell and three gates, namely the input gate, the output gate, and the forget gate.
 300 At these gates, activation functions are utilized. A higher activation rate at the input gate indicates the
 301 need to store the input information in the memory. Conversely, a higher value at the output gate
 302 prompts the stored data release to the subsequent neurons. Lastly, a higher value at the forget gate
 303 eliminates data from the memory units. Although originally designed for neural machine translation,
 304 the Seq-2seq architecture has demonstrated its efficacy in a range of machine learning applications,
 305 such as time series prediction. The Seq-2seq model has modules, including the encoder, intermediate
 306 vector mechanism, and decoder. The input sequences are processed, and features are extracted in the
 307 encoder using LSTM cells. The context vector, which encompasses information from the complete
 308 input data, is derived from the final hidden state. The decoder consists of many LSTM units, with
 309 each unit performing calculations on its hidden state and producing output data. This paper presents a
 310 concept for the utilization of the Seq-2seq model in the prediction of PM concentration.

311 3.3.1. Encoder

312 In a Seq-2seq model, the encoder usually includes one or many LSTM modules. Every unit has
 313 responsibility for processing input sequences, gathering pertinent information, and transmitting it to
 314 the next unit. The mathematical expression that characterizes the functioning of the encoder is as
 315 outlined below:

$$316 \quad hid_t = fn(wt^{hidhid} * hid_{t-1} + wt^{hip} * p_t + b_{hid}) \quad (3)$$

317 In this context, the variable hid_t denotes the hidden state at time step t , p_t represents the input at time
 318 step t , wt^{hihi} represents the weight matrix for the recurrent connections, wt^{hip} represents the weight
 319 matrix for the input connections, and fn represents the activation function.

320 3.3.2. Intermediate Vector

321 In the Seq-2seq model, the decoder component utilizes the final hidden state generated by the encoder
 322 as its beginning hidden state. The intermediate vector, which represents the hidden state, is calculated
 323 using equation (8). The primary objective of the intermediate vector is to integrate the knowledge
 324 acquired from the complete source sequence, serving as the initial hidden state of the decoder.

325 3.3.3. Decoder

326 The system comprises one or many LSTM units. The trailing hidden state is passed to each LSTM
 327 cell, which then creates both the output and the current hidden state. The equation provided was
 328 utilized to calculate the hidden state at the current step t , denoted as hid_t .

$$329 \quad cs_t = fn(wt^{hidhid} * cs_{t-1}). \quad (4)$$

330 The cell state at time step t and the prior time step $t-1$ are denoted as cs_t and cs_{t-1} respectively. The
 331 equation [23] provides the output at each time step.

$$332 \quad O_t = fn(wt^s * cs_t). \quad (5)$$

333 The Softmax function is utilized in the sequence-to-sequence (Seq-2seq) paradigm to produce the
 334 output sequence. Furthermore, it is possible to employ an attention mechanism, such as the Bahdanau
 335 attention mechanism, to capture the correlation between the input and output sequences. This
 336 approach ensures that the input and output sequences are aligned and that important information in the
 337 input sequence is given proper attention throughout the decoding process by giving alignment values.
 338 Through the utilization of attention, the model may choose to concentrate on pertinent segments of the
 339 input sequence, hence enhancing its capacity to produce precise and contextually appropriate output
 340 sequences [24].

$$341 \quad cv_t = \sum_{i=1}^T (\zeta_{ti} * hid_i). \quad (6)$$

342 The context vector at time step t is denoted as cv_t , where T represents the length of the input
 343 sequence. The alignment scores among the current decoder hidden state hid_i and all the encoder
 344 hidden states hid_i are represented as ζ_{ti} .

$$345 \quad \zeta_{ti} = \frac{\exp(es_{ti})}{\sum_{k=1}^T \exp(es_{tk})}. \quad (7)$$

346 Here, es_{ti} denotes the alignment energy score among the current hidden state of the decoder and the i -
 347 th hidden state of the encoder.

$$348 \quad es_{ti} = cv^T * \tanh(wt[cs_{t-1}, hid_i]). \quad (8)$$

$$349 \quad cs_t = \tanh(wt[cs_{t-1}, O_{t-1}, cv_t]). \quad (9)$$

350 The objective of ABFO is to enhance the LSTM's learning rate. To normalize, the moving average of
 351 the gradient square is employed. This allows for the augmentation of the step size under the vanishing
 352 gradient condition, as well as the reduction of the step size for larger gradients.

353 3.4. Adaptive BFO Algorithm for Weight Optimization

354 Initially, a weight selection objective function is established. The training dataset is denoted
 355 as $P_{tr} \in \mathbb{R}^{r \times m}$, where r is the sample size and m represents the number of features. The objective
 356 values that correspond to this are represented as $Q_{tr} \in \mathbb{R}^r$. The proportion among the fitting and
 357 validation sets is determined by the parameter x , which ranges from 0.3 to 0.95. The fitting model is
 358 assigned to the first $r_1 = x \cdot r$ samples of P_{tr} , while the remaining $r_2 = r - r_1$ samples are utilized for
 359 validation. The fitting set is denoted as $P_f \in \mathbb{R}^{r_1 \times m}$, while the validation set is denoted as $P_{va} \in$
 360 $\mathbb{R}^{r_2 \times m}$. The objective values for these sets are $Q_f \in \mathbb{R}^{r_1}$ and $Q_v \in \mathbb{R}^{r_2}$, respectively. It is crucial to
 361 acknowledge that validation plays a significant role in guaranteeing the model's ability to generalize
 362 beyond the training set. This is achieved by separating the fitting set P_f from the weights of the neural
 363 network W , which are directly derived using $M(1:r_1)$ and Q_f . The neural network predictions Q_v for
 364 the validation set P_v are derived using $M(r_1 + 1:r)$ and W . The formula used to compute the mean
 365 absolute error (MAE) between the objective Q_v and the predicted values is as follows:

$$366 \quad MAE = \frac{1}{r_2} \sum_{k=1}^{r_2} |Q_k - \hat{Q}_k|. \quad (10)$$

367 The Mean Absolute Error (MAE) is frequently utilized in machine learning as a loss function,
 368 especially in regression tasks, due to its ability to quantify the average amount of mistakes between
 369 paired observations that reflect the same situation. Let us consider the vector is $[x, v, N]^T$, where N
 370 denotes a vector that encompasses the power values of the neurons in the hidden layer, and c
 371 represents a vector that encompasses the indices of the best activation function chosen from Table 1
 372 for each neuron in the hidden layer. Algorithm 1 presents the approach in the form of an objective
 373 function.

Algorithm 1 Objective function.

Requirement: The vector p , the input data P and the target Q .

1: process objective $\text{fn}(P, Q, p)$

2: Divided p into x, v and N , and set r the rows number of P .

3: Ensure that only the nonnegative elements are retained in N , and in v , keep only their corresponding activation function numbering.

4: Compute the matrix K under the N and v .

5: Set $r_1 = pr, r_2 = r - r_1, P_{fi} = P(1 : r_1, :), Q_{fi} = Y(1 : r_1), P_{va} = P(r_1 + 1 : r, :)$ and $Q_{va} = Q(r_1 + 1 : r)$.

6: calculate Wt utilizing $K(1 : r_1)$ and Q_{fi} by using LSTM.

7 calculate \hat{Q}_{va} utilizing $M(r_1 + 1 : r)$ and Wt .

8: assign the MAE using eqn (10).

9: **end**

374

375 The optimization technique outlined in Algorithm 1 involves the minimization of the objective
 376 function by the utilization of beetle behaviour. The optimization process entails the minimization of
 377 the objective function in relation to a vector $\theta = [x, v^T, N^T]^T$, where x is a parameter and v is a vector
 378 variable consisting of integer values 1, 2, 3, and 4, which correspond to the activation functions
 379 outlined in method 1. Furthermore, it should be noted that the vector N possesses an equivalent
 380 magnitude to that of v , with its elements spanning from 0 to $n_{max} - 1$, where n_{max} represents the
 381 upper limit of hidden layer neurons as determined by the user. The power of the activation functions
 382 for each neuron in the hidden layer is represented by the $n_{max} + 1$ values.

383 In the suggested methodology, the position of the beetle, namely its weight value, is represented by
 384 the vector p . The objective function $f(p)$ in algorithm 1 is used to represent the concentration of odour
 385 at position p . The lowest value of $f(p)$ indicates the origin of the odour. Furthermore, the notation p^t is
 386 employed, where t ranges from 1 to t_{max} , and t denotes the number of iterations. Thus, the lower
 387 bound $L = [0.3, 1^T, 0^T]$, where $1, 0 \in \mathbb{R}^{(n_{max}+1)}$ represents the vectors all-ones and all-zeros,
 388 respectively. The upper boundary, denoted as $(U)=[0.3, 1^T, [4,1]^T \cdot n_{max}]^T$. To make sure that $L \leq$
 389 $p \leq U$ is satisfied, the element-wise function provided for the element $i = 1, \dots, 2n_{max} + 1$ will be
 390 employed.

$$391 \quad g(p_i) = \begin{cases} U_i, & p_i > U_i \\ p_i, & L \leq p_i \leq U \\ L_i, & p_i < L_i \end{cases} \quad (11)$$

392 Therefore, the beetle's chaotic search route defines a model of searching behaviour as follows:

$$393 \quad Cs = \frac{\gamma}{\epsilon + \|\gamma\|^t} \quad (12)$$

394 The expression $\gamma \in Ra^{2n_{max}+1}$ denotes a random vector consisting of $2n_{max} + 1$ elements, while
 395 $\epsilon = 2^{-52}$. The left (p_L) and right (p_R) feeler are created using the following formulae to imitate the
 396 seeking behaviors of the beetle's feeler:

$$397 \quad p_R = g(Ra(p^t + \eta^t Cs)), \quad p_L = g(Ra(p^t - \eta^t Cs)). \quad (13)$$

398 In this context, the sensing breadth of the feeler, denoted as η^t , represents the capability of the exploit
 399 at the t -th instant. Additionally, consider the probable optimal solution (i.e. weight) (p_x):

$$400 \quad p_x = g \left(Ra \left(p^t + \xi^t \eta^t \text{sign}(f(p_L) - f(p_{Ra})) \right) \right), \quad (14)$$

401 The notation ξ^t denotes a step size, which signifies the rate of convergence after an increment in t
 402 during the search procedure. Following this, the behaviour of detection may be characterized as
 403 follows:

$$404 \quad p^{t+1} = \begin{cases} p_x, & f(p_x) \leq f(p^t) \\ p^t, & f(p_x) > f(p^t) \end{cases} \quad (15)$$

405 The subsequent section delineates the updating regulations pertaining to η and ξ .

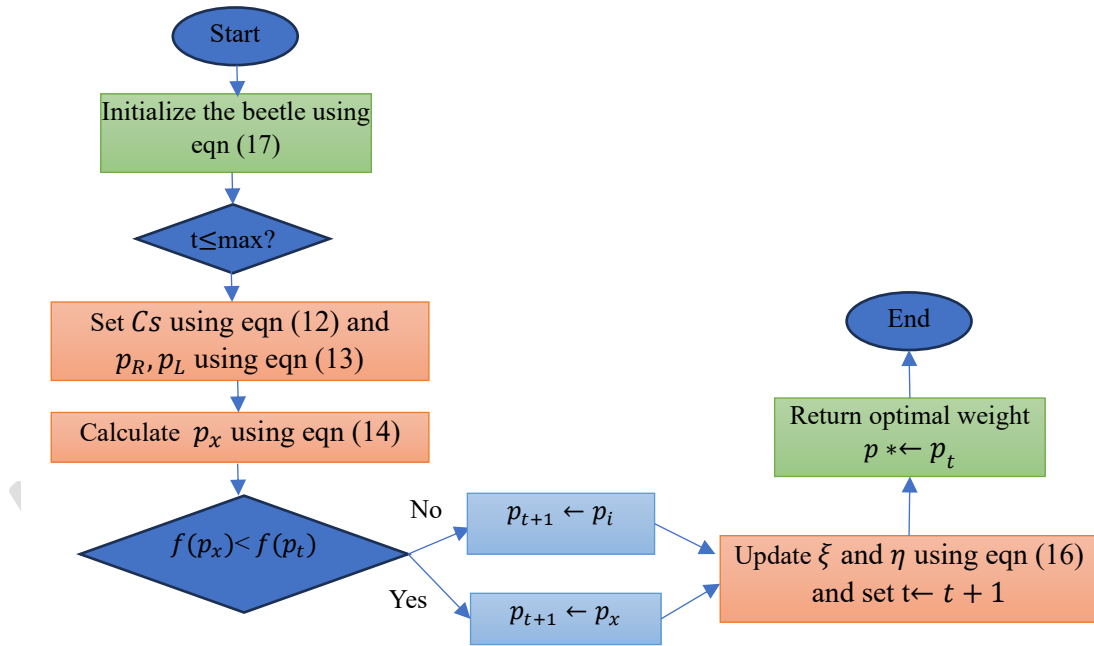
$$406 \quad \eta^{t+1} = 0.991\eta^t + 0.001, \quad \xi^{t+1} = 0.991\xi^t \quad (16)$$

407 The fundamental requirements must be known for the aforementioned methodology are as follows:

$$408 \quad p^0 = [1 - y, 2 - y, \dots, 2n_{\max} + 1 - y]^T, \quad (17)$$

409 Where $y = Ra((2n_{\max} + 1)/2)$.

410 Subsequently, the Seq-2seq LSTM method utilizes the whole training data set to identify and produce
 411 the optimal ratio x^* among the fitting and validation sets, the ideal weight (W_t), the optimal power
 412 value (N^*), and the optimal activation function for each neuron in the hidden layer (v^*). The proposed
 413 algorithm's pseudocode is illustrated in algorithm 2, while the flowchart is presented in Figure 3.



414

415

Figure 3. Flow chart of ABFO for weight selection

Algorithm 2: weight selection for seq-2seq LSTM

Input: objective fn(P, Q, p), utilize the notation p^t , where $t=1,2,3,\dots,t_{\max}$

Output: optimal solution

Initialize the beetle using eqn (17)

While($t \leq \max?$)

Set C_s using eqn (12) and p_R, p_L using eqn (13)

Calculate p_x using eqn (14) Update the value

If $f(p_x) < f(p_t)$ then
 Update $p_{t+1} \leftarrow p_t, p_{t+1} \leftarrow p_x$
 Update ξ and η using eqn (16) and set $t \leftarrow t + 1$ potential solution
 Return optimal weight $p^* \leftarrow p_t$
 The best solution is considered for Optimal weight in seq-2seq LSTM.
 End

416

417 4. RESEARCH RESULTS ANALYSIS AND DISCUSSION

418 4.1. Experimental Setup

419 To assess the superiority and generalization of the method proposed seq-2seq LSTM in this
 420 paper for long-term prediction, comparative experiments were conducted using several control
 421 groups, including the general GRU module, the informer model (known for its superior short-term
 422 forecasting capabilities), the Autoformer method, and a model combining empirical mode
 423 decompositions with the GRU module (modal GRU). The completed dataset was divided into a
 424 training dataset comprising 85% of the data and a test dataset comprising the remaining 15%. For the
 425 models using non-modal decomposition and those employing modal decomposition, automatic
 426 parameter adjustment functions were incorporated. The key difference lies in the timing of parameter
 427 adjustment: for the non-modal decomposition model, adjustment happens after every prediction
 428 process completes, whereas, for the modal decomposition model, modification takes place after the
 429 predictions of all the components. Initial settings of parameters were based on the features of various
 430 models for hyperparameter tuning. The proposed seq-2seq LSTM performance is evaluated and the
 431 performance is compared with existing STA-ResCNN [8], CNN-LSTM [11] and LSTM [16] schemes.
 432 In the experiment, the model hyperparameters are configured as follows: The training process
 433 comprises 1,000 iterations with a batch size of 128 and a rejection rate set at 0.1. The model
 434 architecture includes GRU (Gated Recurrent Unit) layers with 64 hidden units, and the input data
 435 incorporates sequences of eight long-term historical data points. Training is facilitated using the Adam
 436 optimizer, with the MSE serving as the chosen loss function. The total objective function aims to
 437 minimize the MSE across the training iterations, thus optimizing the model's predictive performance.

$$438 \quad O(X^{t \sim t+k}, \hat{X}^{t \sim t+k}) = \frac{1}{N_s} \sum_{i=1}^{N_s} (X^{t \sim t+k}, \hat{X}^{t \sim t+k}) \quad (18)$$

439 Where N_s was the total training samples. Three parameters were utilized to compute the differences
 440 among the actual value \hat{X}_t of PM2.5 and the projected value X_t . The PM2.5's mean value was
 441 defined as \bar{X} , which includes:

$$442 \quad RMSE = \sqrt{\frac{1}{n} \sum_{i=1}^n (X_t - \bar{X}_t)^2} \quad (19)$$

$$443 \quad MAE = \frac{1}{n} \sum_{i=1}^n |X_t - \bar{X}_t| \quad (20)$$

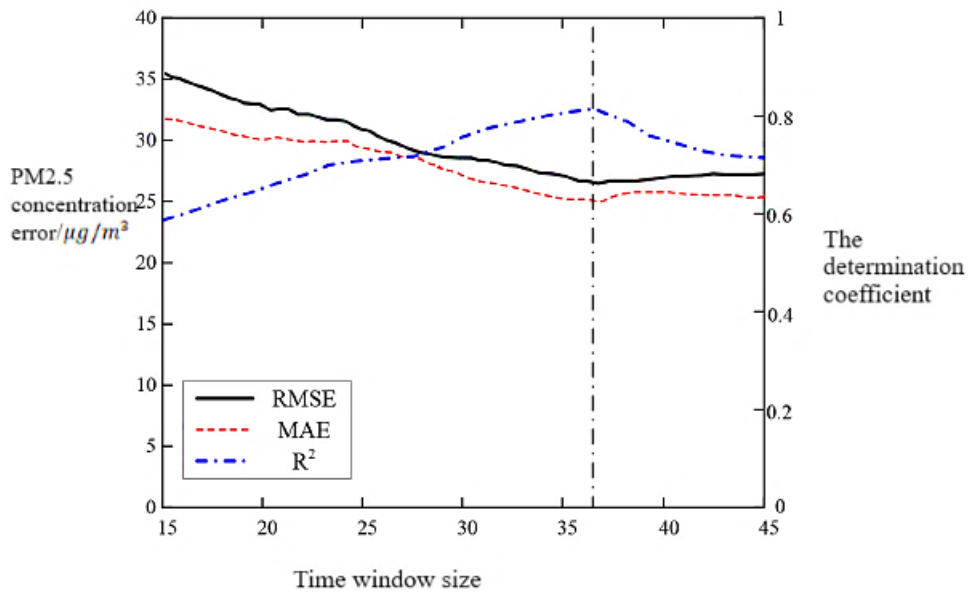
$$444 \quad R^2 = 1 - \frac{\sum_{i=1}^m (X_t - \bar{X}_t)^2}{\sum_{i=1}^m (X_t - \bar{X}_t)^2} \quad (21)$$

445 Among these metrics, MAE and RMSE were employed to quantify the disparity among the original
 446 and predicted values. RMSE indicates the model's sensitivity to huge errors, while MAE indicates its
 447 reliability. Smaller values of both RMSE and MAE signify better predictive performance.
 448 Additionally, R^2 the predictive accuracy of the model relative to the actual data. A higher R^2 value
 449 indicates a more effective forecasting outcome.

450 4.2. Comparison of Different Time Window Sizes for PM Concentrations 2.5 and 10

451 PM2.5 and 10 concentration data are influenced by various relevant time series, although
 452 variations in all the time series values do not impact the PM2.5 concentration values. This indicates a
 453 lag effect, where the variable value at the previous moment affects the PM2.5 concentration values at

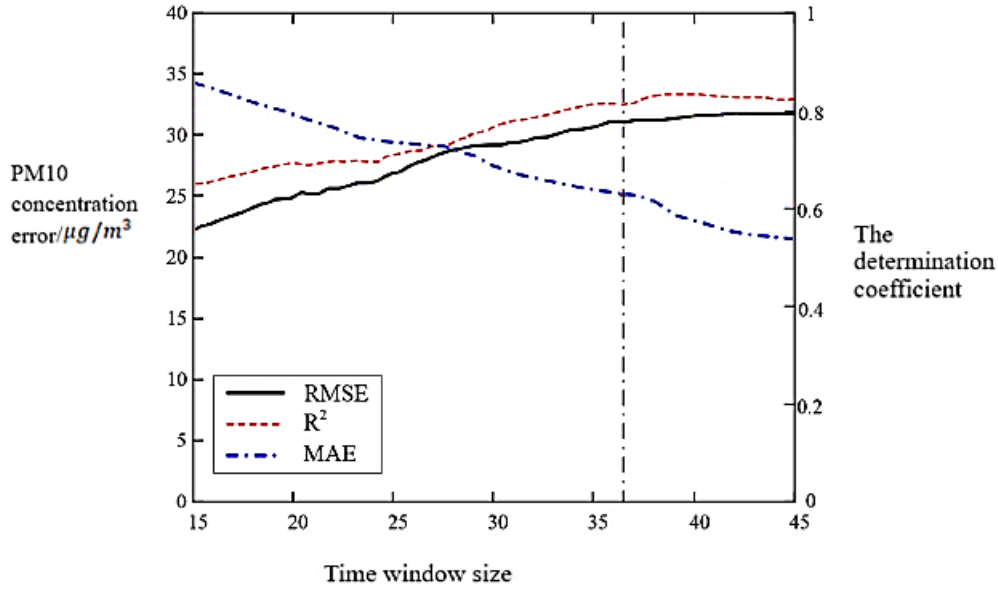
454 the following moment with a lag. While the lag effect might be pronounced in the short period, it
455 diminishes in the long term.



456

457 **Figure 4. Different Time Window Sizes Performance for PM Concentrations 2.5**

458 A smaller window size may not provide sufficient long-term memory input for the Seq-2seq LSTM
459 model, while a larger window size may introduce irrelevant information, increasing unnecessary
460 computational complexity. Hence, determining the optimal window size is crucial. A sliding window
461 strategy was employed to create relative time series samples for all the records. To establish a suitable
462 historical time window size, various values from the candidate sets [12, 16, 20, 24, 28, 32, 36, 40, 44]
463 are selected. The changes in MAE, RMSE, and R^2 of the research model were depicted in Figures 4
464 and 6 for PM 2.5 and 10 to guide the selection process. As illustrated in figure 4 and 5, if the size of
465 the window was less than 36, both the MAE and RMSE evaluations decreased while the R^2
466 evaluation value improves with increasing window size. This trend is attributed to the limited
467 historical feature information inputted to the model when the window size is too small, resulting in
468 lower prediction performance. Conversely, as the size of the window increases gradually, the research
469 model receives more historical data as input, enabling it to capture additional nonlinearities and
470 dependencies within the sequence, thereby enhancing predictive ability. However, when the size of
471 the window surpasses 36, the values of MAE and RMSE start to increase, while the evaluation value
472 of R^2 decreases before stabilizing. This phenomenon occurs due to the excessive input of unnecessary
473 information with larger window sizes, leading to increased noise and interference with the model's
474 performance. Consequently, in the experiment, the historical time window size was set to 36 to
475 achieve the optimal balance between capturing relevant historical features and mitigating noise
476 interference.



477

478 **Figure 5. Different Time Window Sizes performance comparison for PM concentrations 10**

479 The overall performance of the proposed scheme in terms of RMSE, MAE and R^2 are depicted in
 480 table 2. It shows the performance numeric evaluation and is compared with the current scheme's
 481 numeric values. It shows the proposed seq-2seq LSTM attained better performance results compared
 482 to current schemes. The proposed seq-2seq LSTM models are relatively easier to train and tune
 483 compared to complex convolutional architectures like STA-ResCNN. This simplicity in model design
 484 and training process may lead to faster convergence and better generalization performance and it's
 485 known for their ability to handle noisy data and missing values effectively. LSTM's robustness to
 486 such noise can result in more reliable predictions compared to STA-ResCNN.

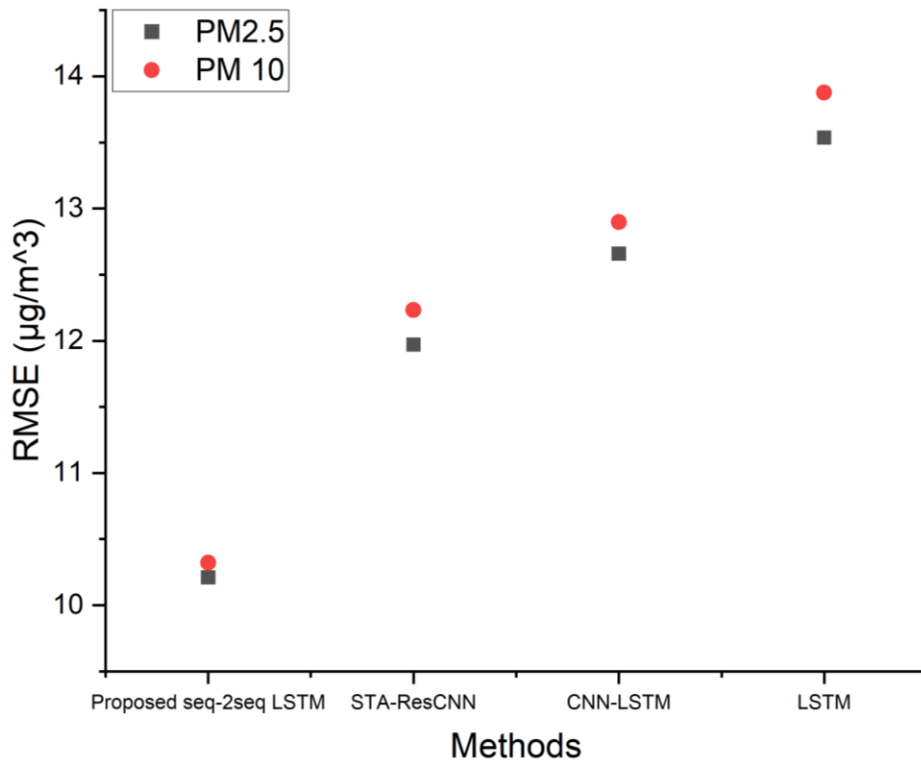
487 **Table 2. Overall Performance Comparison Among PM Concentration Prediction Schemes**

Methods	RMSE ($\mu\text{g}/\text{m}^3$)		MAE ($\mu\text{g}/\text{m}^3$)		R^2	
	PM 2.5	PM 10	PM 2.5	PM 10	PM 2.5	PM 10
Proposed seq-2seq LSTM	10.211	10.321	5.641	5.764	0.976	0.945
STA-ResCNN	11.971	12.232	6.938	7.24	0.828	0.834
CNN-LSTM	12.659	12.896	7.296	7.542	0.762	0.745
LSTM	13.536	13.876	7.781	8.122	0.668	0.675

488

489 **4.3. RMSE performance comparison**

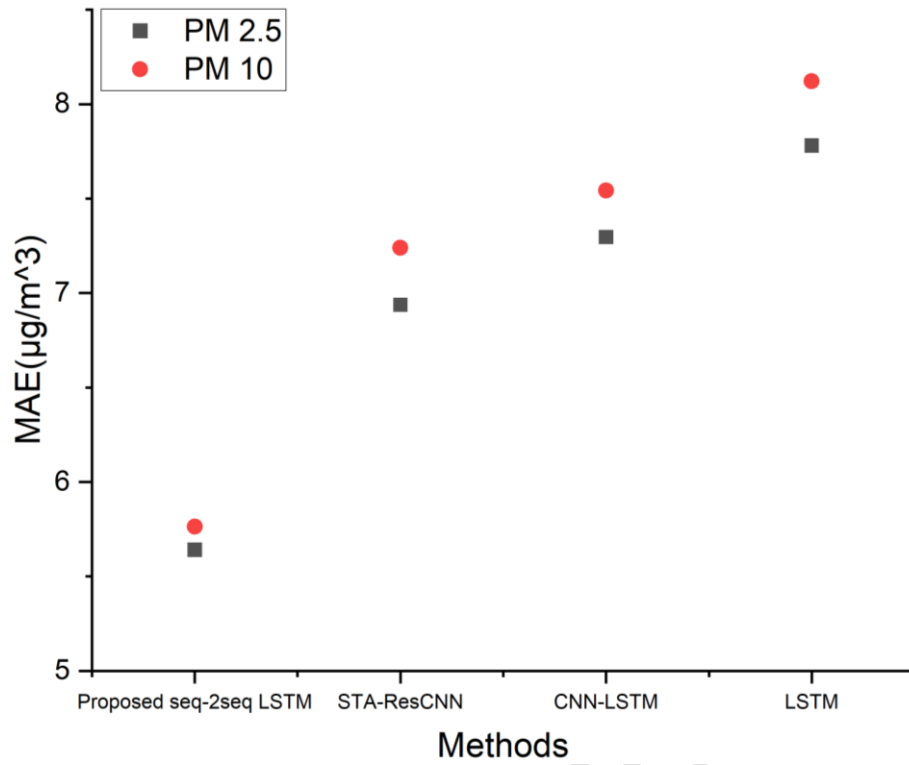
490 Figure 6 shows the RMSE performance comparison among the proposed seq-2seq LSTM
 491 model and compared with existing PM concentration prediction schemes like STA-ResCNN, CNN-
 492 LSTM and LSTM. It shows the RMSE of proposed and existing schemes for PM 2.5 and PM 10, and
 493 the results show that the proposed scheme attained less RMSE compared to others. The proposed seq-
 494 2seq LSTM is designed to handle sequential data with varying lengths and time lags. PM
 495 concentration prediction involves forecasting future values based on historical observations, which
 496 aligns well with the sequential nature of LSTM models. The model's ability to retain relevant
 497 information over time enables it to make accurate predictions, resulting in lower RMSE. As well as it
 498 has a high capacity to learn complex temporal patterns present in PM concentration data. They can
 499 capture both short-term fluctuations and long-term trends, allowing them to adapt to the dynamic
 500 nature of air quality data. This capacity to learn intricate patterns contributes to the model's ability to
 501 achieve lower RMSE.



502
503 **Figure 6. RMSE performance comparison among PM concentration schemes**

504 **4.4. MAE performance comparison**

505 Figure 7 shows the MAE performance comparison among the proposed seq-2seq LSTM
 506 model and compared with existing PM concentration prediction schemes like STA-ResCNN, CNN-
 507 LSTM and LSTM. It shows the MAE of proposed and existing schemes for PM 2.5 and PM 10, and
 508 the results show that the proposed scheme attained less MAE compared to others. The proposed
 509 model has a high capacity to learn complex relationships between input features and target variables.
 510 PM concentration prediction often involves capturing intricate relationships between various
 511 environmental factors, such as weather conditions, geographic features, and pollutant emissions. The
 512 LSTM's ability to learn these relationships can lead to more accurate predictions and hence lower
 513 MAE. As well as it offers interpretability by allowing analysts to understand the importance of
 514 different features in predicting PM concentrations. PM concentration data may have irregular time
 515 intervals between observations due to factors such as sensor sampling frequency or data collection
 516 schedules. The proposed seq-2seq LSTM model can handle irregular time intervals effectively,
 517 allowing them to maintain predictive accuracy without requiring interpolation or resampling of the
 518 data.



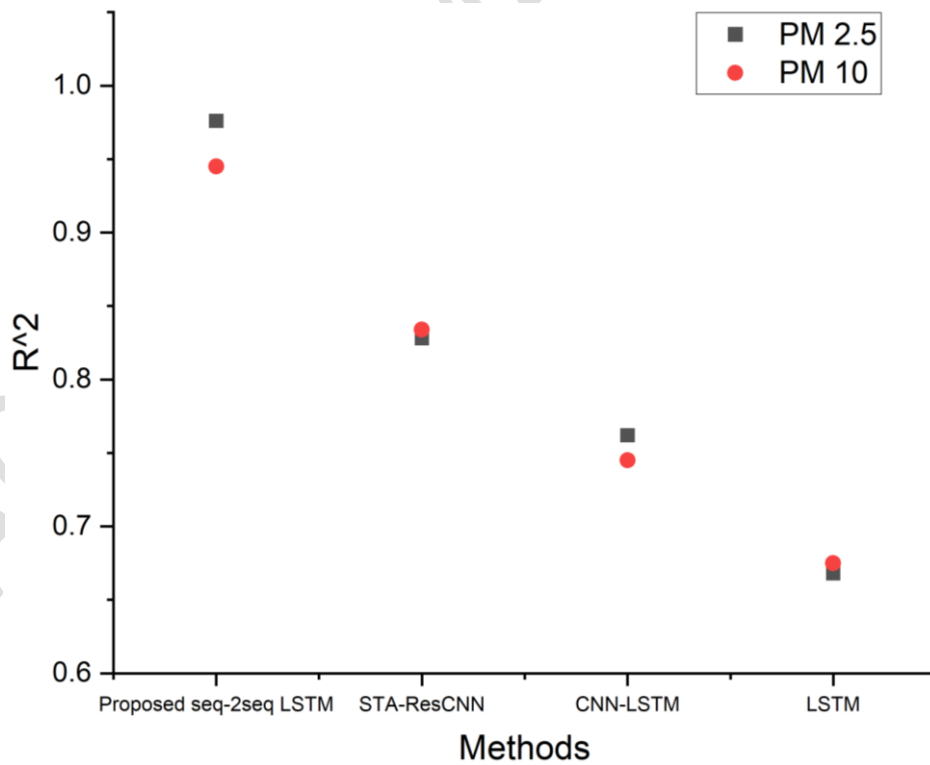
519

520

Figure 7. MAE performance comparison among PM concentration schemes

521

4.5. R^2 performance comparison



522

523

Figure 8. R^2 Performance comparison among PM concentration schemes

524

525

526

Figure 8 shows the R^2 performance comparison among proposed seq-2seq LSTM model and compared with existing PM concentration prediction schemes like STA-ResCNN, CNN-LSTM and LSTM. It shows the MAE of proposed and existing schemes for PM 2.5 and PM 10, and the results

527 show that the proposed scheme attained high R^2 compared to others. PM concentration data may have
528 irregular time intervals between observations due to factors such as sensor sampling frequency or data
529 collection schedules. The proposed model can handle irregular time intervals effectively, allowing
530 them to maintain predictive accuracy without requiring interpolation or resampling of the data. This
531 flexibility in handling irregular time intervals contributes to higher R^2 values. As well as it is known
532 for its capability for generalizing well to unknown data. By capturing initial data patterns, it can make
533 predictions accurately even on data points not seen during training, leading to R^2 values on test or
534 validation datasets. For the above reasons, the proposed scheme attained better performances
535 compared to others.

536 The proposed model offers significant advantages in air pollutant concentration prediction, exhibiting
537 improved accuracy and strong predictive capability compared to existing models. By integrating
538 advanced techniques such as Modal Autoformer and Seq-2Seq LSTM, the model achieves
539 comprehensive forecasting by capturing detailed variations in atmospheric conditions. However,
540 computational complexity and potential challenges in model interpretability may limit its scalability
541 and utility in decision-making processes. The limitation of the research is its dependence on the Indian
542 air quality dataset, which could limit the model's generalizability to regions with different atmospheric
543 conditions and pollutant sources. As compared to the current models results, the developed research
544 model has gained lower RMSE and MAE, and better R^2 results. However, there is potential to
545 improve the results by capturing variations in concentrations of PM. The obtained results indicate that
546 the research model's predictive capability could slightly reduce in highly or extreme dynamic weather
547 conditions. Additionally, the computational complexity of integrating Modal Auto-former and Seq-
548 2Seq LSTM networks, along with ABFO optimization, could pose challenges for real-time
549 applications in resource-constrained environments. Additionally, the model's performance could be
550 perceptive to the quality and integrity of input data, requiring robust preprocessing and handling of
551 missing values for accurate predictions. Addressing these limitations through further research and
552 refinement could enhance the model's applicability in real-world air quality forecasting scenarios.

553 5. CONCLUSION

554 This research presented a novel system for predicting PM_{2.5} and PM₁₀ concentration levels
555 by combining a Modal Autoformer with the Seq-2Seq predictive model. The Seq-2Seq model
556 employed sequential learning and square transformation methods to improve accuracy in
557 concentration prediction, while the integration of a Modal Autoformer capture subtle variations in
558 atmospheric conditions. The developed model optimized by the ABFO algorithm exhibited enhanced
559 performance relative to conventional techniques. The optimized research model was validated through
560 extensive testing with Air Quality Data from Kaggle repository. The results demonstrated the model's
561 potential for accurate forecasting of PM_{2.5} and PM₁₀ concentrations with significant implications for
562 air quality management and public health activities. The Proposed seq-2seq LSTM model achieved
563 10.211 RMSE for PM_{2.5}, 10.321 RMSE for PM₁₀, 5.641 MAE for PM_{2.5}, 5.764 MAE for PM₁₀,
564 0.976 R^2 for PM_{2.5}, and 0.945 R^2 for PM₁₀. The achieved results demonstrated the proposed
565 model's superiority in PM_{2.5} and PM₁₀ concentration prediction compared to existing methods. This
566 was evidenced by lower RMSE and MAE values, alongside higher R^2 scores, signifying enhanced
567 accuracy and predictive power.

568 In future, the research will investigate additional enhancements to the predictive model, such as
569 incorporating attention mechanisms or exploring alternative deep learning architectures to capture
570 complex patterns in the data more effectively. The research will focus on improving the
571 generalizability by evaluating various datasets with different atmospheric conditions. Further the
572 research will address the data quality issues with advanced preprocessing methods and the model can
573 be optimized with advanced optimization technique for enhancing overall prediction accuracy.

574 **Declarations:**

575 **Acknowledgements**

576 Not applicable

577 **Contributions**

578 All authors have made substantial contributions to conception and ideas. All authors participated
579 actively in the interpretation of data. This manuscript was initially prepared by the corresponding
580 author and critically reviewed by the other co-authors. All the authors have revised and approved the
581 final version of the manuscript.

582 **Ethics approval statement**

583 Not applicable

584 **Competing Interests**

585 The authors declare no competing interests.

586 **Funding**

587 There was no external/internal funding for this study.

588

589 **References**

- 590 Ahmad, W., Arulkumar, V., Parthiban, K., Bhuvaneswari, E., Arif, M., & Guruprakash, K. S. (2024).
591 Convergence of Modern Technologies for Data Architectures. In *Wireless Communication*
592 *Technologies*, CRC Press, **26**, 82-100.
- 593 B. Deep, I. Mathur, N. Joshi, An approach to forecast pollutant concentrations with varied dispersions,
594 *Int. J. Environ. Sci. Technol.* **19** (2022) 5131e5138.
- 595 B. Peralta, T. Sepúlveda, O. Nicolis, L. Caro, Space-Time Predictions of PM_{2.5} Concentration in
596 Santiago de Chile Using LSTM Network, *Appl. Sci.* **12**, 113-127.
- 597 C. Wang, J. Zhang, J. Du, G. Wang, J. J. Klemes, B. Wang, Q. Liao, Y. Lang, Weather conditions-
598 based hybrid model for multiple air pollutant forecasting and minimisations, *J. Clean. Prod.*
599 (2022), **352**, 131-143.
- 600 Chen, L., Cui, B., Zhang, C., Hu, X., Wang, Y., Li, G., Chang, L., & Liu, L. (2024). Impacts of Fuel
601 Stage Ratio on the Morphological and Nanostructural Characteristics of Soot Emissions from a
602 Twin Annular Premixing Swirler Combustor. *Environmental Science & Technology*, **58**, 10558–
603 10566.
- 604 Ding, C et al., 2021. A hybrid CNN-LSTM model for predicting PM_{2.5} in Beijing based on
605 spatiotemporal correlations. *Environ. Ecol. Stat.*, **28**, 503-522.
- 606 Dun, Y. Yang, F. Lei, A novel hybrid model based on spatiotemporal correlations for air quality
607 predictions, *Mobile Inf. Syst.*, **23**, 156-172.
- 608 Faraji, M., Nadi, S., Ghafarpasand, O., Homoyoni, S., Downey, K., 2022. An integrated 3D CNN-
609 GRU deep learning methods for short-term predictions of PM_{2.5} concentrations in urban
610 environments. *Sci. Total Environ.*, **834**, 155-324.

611 Gong, H., Hu, J., Rui, X., Wang, Y., & Zhu, N. (2024). Drivers of change behind the spatial
612 distribution and fate of typical trace organic pollutants in fresh waste leachate across China.
613 *Water Research*, **263**, 122170.

614 Gul, S., Khan, G. M., & Yousaf, S. (2022). Multi-steps short-term PM 2.5 forecasting for enactments
615 of proactive environmental regulations strategies. *Environmental Monitoring and Assessments*,
616 **194**, 386-398.

617 K. H. Wasim, H. Mushtaq, F. Abid, A. M. A. Mahfouz, A. Shaikh, M. Turan, J. Rashid, Forecasting of
618 air quality using an optimized recurrent neural networks, *Processes*, **10**, (2022), 239-253.

619 K. Zhang et al., Multi step forecasts of PM2.5 and PM10 concentration using convolutional neural
620 networks integrated with spatialetemporal attentions and residual learning, *Environ. Int.* **171**,
621 345-367.

622 L. Shi et al., A balanced social LSTM for PM2.5 concentrations predictions based on local
623 spatiotemporal correlations, *Chemosphere*, **291**, 133-144,

624 Li, C., Hamer, M. S., Zheng, B., & Cohen, R. C. (2022). Accelerated reductions of air pollutant in
625 China, 2017-2020. *Science of the Total Environments*, **803**, 187-211.

626 Lin, Y. C. et al., (2020). Chemical characterizations of PM2.5 emission and atmospheric metallics
627 elements concentration in PM2.5 emitted from mobile sources gasoline-fueled vehicle. *Science*
628 *of the Total Environments*, **739**, 237-252.

629 Liu, Y., Zhou, Y., & Lu, J. (2020). Exploring the relationships between air pollutions and
630 meteorological condition in China under environmental governances. *Scientific report*, **10**, 235-
631 276.

632 M. A. A. Al-qaness, H. Fan, A. A. Ewees, D. Yousri, M. A. Elaziz, (2021) Improved ANFIS models
633 for forecasting Wuhan City Air Quality and analysis COVID-19 lockdown impact on air quality,
634 *Environ. Res*, **194**, 543-562,

635 M. Yu, A. Masarur, C. B. Boxe, (2023) Predicting hourly PM2.5 concentration in wildfires-prone area
636 using a Spatio Temporal Transformers model, *Sci. Total Environ.* **860**, 345-364.

637 Mapok, A., Hyde, K. D., Hasan, K., Kemkuigno, B. M., Čamoková, A., Surup, F., ... & Stadler, M.
638 (2022). Ten decadal advances in fungal biology leading toward human well-being. *Fungal*
639 *Diversity*, **116**, 547-614.

640 Meng, S., Zhang, C., Shi, Q., Chen, Z., Hu, W., & Lu, F. (2023). A robust infrared small target
641 detection method jointing multiple information and noise prediction: Algorithm and benchmark.
642 *IEEE Transactions on Geoscience and Remote Sensing*, **61**, (1-17).

- 643 Pruthi, D., & Liu, Y. (2022). Low-cost natures-inspired deep learning systems for PM2.5 forecasts
644 over Delhi, India. *Environment International*, **166**, 107373.
- 645 Sutskever, O. Vinyals, and Q. V. Le (2014), "Sequences to sequence learning with neural network," In
646 *Advance in neural information processing systems*, NIPS, Cambridge, MA, United States: MIT
647 Press,**12**, (3104–3112).
- 648 W. Ding, Y. Zhu, Predictions of PM2.5 concentrations in ningxia hui autonomous regions based on
649 PCA-attentions-LSTM, *Atmosphere*, **13**, 143-168.
- 650 X. Wu, C. Zang, J. Zhu, X. Zang (2022), Research on PM2.5 concentrations predictions based on the
651 CE-AGA-LSTM models, *Appl. Sci*, **12**, 7009.
- 652 Xu, Z., Wang, M., Chang, L., Pan, K., Shen, X., Zhong, S., Xu, J., Liu, L., Li, G., & Chen, L. (2024).
653 Assessing the particulate matter emission reduction characteristics of small turbofan engine
654 fueled with 100% HEFA sustainable aviation fuel. *Science of The Total Environment*, **945**,
655 174128.
- 656 Yang, B. Y., Fan, S., Thiering, E., Seisler, J., Nowak, D., Dong, G. H., & Heinrich, J. (2020), Ambient
657 air pollutions and diabetes: a systematic review and meta-analysis. *Environmental Research*, **180**,
658 (138-153).
- 659 Yu, C. H. et al., (2016). A novel mobile monitoring approach to characterize spatial and temporal
660 variations in traffics-related air pollutant in an urban community. *Atmospherics Environment*,
661 **141**, (161-173).